ANALYSIS OF FLOW AND THERMAL PHENOMENA IN EVACUATED TUBE COLLECTORS

Anna DEMIANIUK*, Sławomir Adam SORKO*

*Faculty of Environmental Engineering, Department of Heat Engineering, Bialystok University of Technology, ul. Wiejska 45 E, 15-351 Białystok, Poland

a.b.demianiuk@10g.pl, s.sorko@pb.edu.pl

Abstract: The subject of this case study is an issue of optimisation of flat tube solar collectors. Basic elements of energy analysis of performance parameters described by Hottel-Whillier equation are presented in the article. It is considered to be crucial to precisely analyse fluid flow through flow elements in evacuated tube collectors. It is especially important in the case of systems with channels of cross-sections shapes different from circular and for the use of detailed mathematical description of complex film conduction phenomena. It is presented that the advanced analysis of the flow and thermal phenomena in complex heat transfer systems, represented by evacuated tube collectors, enables engineering rationalisation of technical solutions for these devices.

Keywords: Flat Plate Solar Collector, Heat Transfer, Fluid Flow in Pipes, Optimum Mass Flow Rate, Boundary Equation Method

1. INTRODUCTION

The primary objective of every active and passive solar system is to gain solar radiation energy and to transfer it to the recipient in a planned, relatively simple way with highest possible efficiency of conversion. In many active and passive solar systems the basic element that absorbs solar energy is a flat plate collector. Its basic element is a plate or tube absorber. In the case of the plate absorber the medium which receives the heat flows directly under the absorber surface. The heat absorbing medium can be a liquid as well as a gas. The majority of collectors' solutions employ tube absorbers, where tubular elements are attached to the absorber plate. Pipes are arranged parallel to each other forming series of channels. In majority of installation solutions pipes or channels are filled up with a liquid, whereas in passive systems, typically, the air is the medium. Another form of tube collectors are evacuated tube collectors. In this particular type of solution pipes transporting heat are placed inside glass vacuum pipes in order to reduce heat loss from the medium to the ambient (Chwieduk, 2011 and Kalogirou, 2004). In the advanced constructions, designed for conversion of solar radiation energy into useful energy, panels of photovoltaic cells are placed on the absorber surface. In these cells types (PV/T) solar radiation energy is converted into heat and electricity in the rate dependent on the construction of the device (Ibrahim et al. 2011)

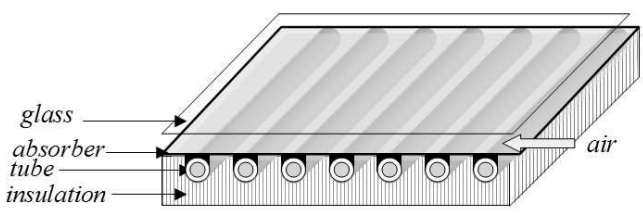

Fig. 1. Flat plate liquid collector with circular cross-section tubes

Variations design versions and types of solar collectors depending on kind of application (passive and active systems), type of medium used (air and liquid), connections for photovoltaic modules, and applied materials are described in detail in the literature (Zondag, 2008; Zhang et al., 2012; Charalambous et al., 2007).

The cross-section of flat plate liquid collector is presented in Fig. 1.

2. COLLECTOR HEAT BALANCE EQUATION

Deliberation on the thermal phenomena occurring in the collector is based on its thermal balance calculation. Balance equations of the configuration absorber-pipe system in the simplest form are obtained having analysed heat fluxes in the plate of the absorber and heat flux transferred to the medium inside pipe system of the collector. Fig. 2 presents a cross-section of flat plate collector with circular pipes system.

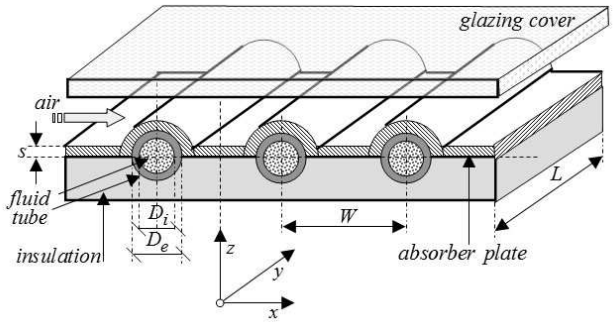

Fig. 2. The layout of a flat plate liquid collector of various dimensions

As investigated by Luminosu and Fara (2005) as well as Farahat et al., (2009), one of the most effective ways to obtain

the highest possible efficiency of the collector operation is to reduce heat loss to a minimum. Therefore it is crucial that thermal resistance of elements separating the main body of the solar radiation receiver, i.e. the absorbing surface (absorber), from the ambient was possibly the highest (Vestlund et al., 2009). Additionally, when absorbing surface is taken into consideration it is necessary to intensify processes of heat transfer in the absorber. It is important that the thermal resistance is possibly the lowest across absorber plate (between pipes or channels) and between the plate and the pipe or channel. A heat transfer phenomenon that occurs when the solar radiation energy is absorbed on the panel of the absorber and during its transfer to the medium flowing in pipe elements is analysed below.

Application of Hottel-Whillier model (Zondag, 2008, Alvarez et al., 2010 and Herrero Martín et al., 2011) in order to analyse thermal processes occurring in the collector facilitates describing temperature distribution $T_p \equiv T_p(x)$ in absorber plate and liquid temperature $T_f \equiv T_f(y)$ inside pipe system of the collector with equations:

$$\frac{\partial^2 T_p(x)}{\partial x^2} - C_p T_p(x) = -C_p\left(T_a + \frac{G_{sa}}{U_L}\right), \tag{1a}$$

where $c_p = \frac{U_L}{\lambda_p \delta}$ with boundary conditions:

$$T_p(x)\Big|_{X=0} = 0 \quad ; \quad T_p(x)\Big|_{X=h=\frac{(W-D_e)}{2}} = T_b \tag{1a*}$$

$$\frac{\partial T_f(y)}{\partial y} - C_f T_f(y) = C_f\left(T_a + \frac{G_{sa}}{U_L}\right) \tag{1b}$$

where $C_f = \frac{nWU_o}{\dot{m}c_p}$

with the boundary condition:

$$C_f = \frac{nWU_o}{\dot{m}c_p} \quad T_f(y)\Big|_{y=0} = T_i \tag{1b*}$$

where: U_L – overall collector heat loss coefficient [W/(m2K)], U_0 – coefficient of heat loss between ambient air and the medium inside pipes of the collector, G_{sa} – solar irradiation [W/m2], T_a – temperature of the ambitne [K], $\dot{m}$ – fluid mass flow rate in pipe collector [kg/s], c_p – heat capacity of fluid [J/(kg K)], λ_p – transmittance of the material [W/(m K)], δ – fin thickness [m], W – tube spacing [m], n – number of pipes in flat plate collector [-], T_b – temperature in the contact area for plate of the absorber and tube element [K], T_i – liquid temperature in the inlet to collector pipe [K].

Solution of the above equations provide to relations which describe temperature distribution in the absorber plate and in the medium flowing through the pipe elements:

$$T_p(x) = \frac{\cosh(C_p x)\left(T_b - T_a + \frac{G_{sa}}{U_L}\right)}{\cosh(C_p h)} + T_a + \frac{G_{sa}}{U_L} \tag{2}$$

Introducing F_R heat-removal factor for the collector:

$$F_R = \frac{\dot{m}c_p(T_o - T_i)}{S_c\left(G_{sa} - U_L(T_i - T_a)\right)} \tag{3}$$

where: S_c – area of the collector [m^2], $T_0 = T_f(y = L)$ – temperature of the medium in the outlet of the collector pipe obtained by calculation from equation (2b).

Density of energy gained by the collector and its useful thermal power can be described by following equations:

$$q_u = F_R\left(G_{sa} - U_L(T_i - T_a)\right) \; q_u = F_R\left(G_{sa} - U_L(T_i - T_a)\right) \tag{4a}$$

$$Q_u = S_c \cdot q_u \tag{4b}$$

Relating the density of the energy converted by the collector defined by Eq. 4a to the solar irradiation the expression determining efficiency of energy generation by the solar collector is as follows:

$$\eta_{c\,th} = \frac{q_u}{G_{sa}} \tag{5}$$

Fluid mass flow rate through system of pipes of the collector is a significant factor. This factor determines solar collector energetic parameters along with the thermal properties of the materials that the absorber is made of, pipe system, medium and with temperature difference between the medium and the ambient air.

Determination of the fluid mass flow of the medium inside the pipe system of the collector is easy in the case when the cross-section of pipes is circular.

In Fig. 3 the tube collectors are presented. There are three options of the cross-section shapes – elliptic, triangular and rectangular. Canals depending on the various construction solutions can be of various arbitrary cross-section shapes which can be obtained by profiling flow systems from steel sheets.

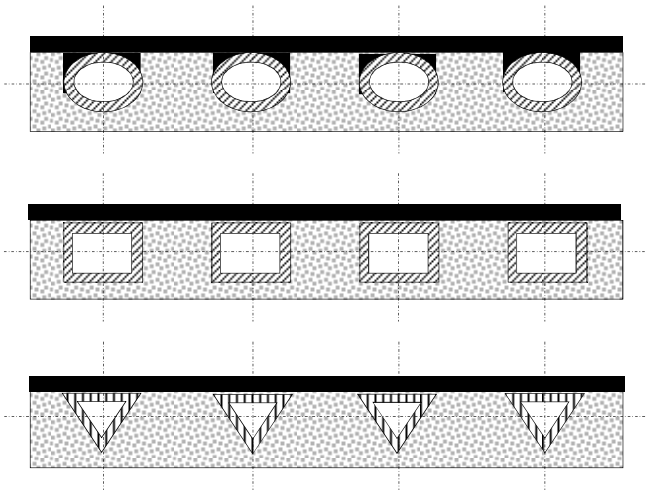

Fig. 3. Flat plate liquid collector with non-circular shape tubes

In the case when the collector pipes cross-sections are different from circular it becomes necessary to determine the flow velocity field and to calculate mass and volume flow rate of the medium by integration of velocity distribution inside the area. The area of calculations is described by canal profile contour. These calculations are essential in order to optimise construction parameters of the collector.

3. FLOW THROUGH NON-CIRCULAR CROSS-SECTION SHAPE PIPES COLLECTOR DETERMINATION

The sufficient model for fluid flow through pipes or hydraulic ducts of the collector flow system is the model of steady, uniform unidirectional laminar flow of incompressible viscous fluid (Batchelor, 1967).

3.1. Flow problem formulation

Unidirectional, slow flow of viscous fluid through a straight-axis pipe in the cross-section (Λ) of arbitrary shape inside the borderline (L), can be described by Stokes' equation with boundary condition which is the assumption of zero velocity value at inflexible and impermeable material border (at the duct partition):

$$\left(\frac{\partial^2 c_z}{\partial x^2}+\frac{\partial^2 c_z}{\partial y^2}\right)=-\Delta P\,, \tag{6}$$

where: $\dfrac{1}{\mu}\dfrac{\partial p}{\partial z}=-\Delta P$

with boundary condition:

$$c_z(x,y)=0 \;\;;\;\; \forall (x,y)\in L \tag{6a}$$

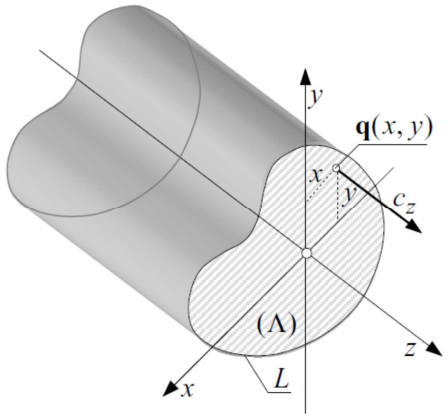

Fig. 4. Unidirectional flow through a straight duct

Among methods of solving the above-formulated boundary problem for Poisson equation (6) there is the decomposition of function ($c_z(x,y)$) into the homogeneous part ($\bar{c}_z(x,y)$), which satisfies Laplace equation, and the non-homogeneous part ($\tilde{c}_z(x,y)$), which satisfies Poisson equation.

$$c_z(x,y)=\bar{c}_z(x,y)+\tilde{c}_z(x,y)\,, \tag{7}$$

where:

$$\nabla^2\bar{c}_z(x,y)=0\,,\qquad \forall (x,y)\in\Lambda\cup L\,, \tag{7a}$$

$$\nabla^2\tilde{c}_z(x,y)=-\Delta P\,,\;\; \forall (x,y)\in\Lambda\cup L\,, \tag{7b}$$

where its non-homogeneous part can be written:

$$\tilde{c}_z(x,y)=-\Delta P\,\upsilon(x,y)\,, \tag{8}$$

where $\upsilon_z(x,y)$ is arbitrary chosen function which satisfies Poisson equation.

$$\nabla^2\upsilon(x,y)=1\;,\;\; \forall (x,y)\in\Lambda\cup L\;. \tag{8a}$$

One of the possible forms of this function is the square of the radius vector of any point $\mathbf{q}\equiv\mathbf{q}(x_\mathbf{q},y_\mathbf{q})\in\Lambda\cup L$,(Batchelor, 1967) i.e.:

$$\upsilon(\mathbf{q})=\frac{1}{4}r^2(\mathbf{q}) \tag{8a*}$$

Given the decomposition (7) of function $c_z(x,y)$ boundary condition $c_z(x,y)=0\;;\;\forall(x,y)\in L$ takes the form:

$$\bar{c}_z(x,y)=-\tilde{c}_z(x,y)=\Delta P\,\upsilon(x,y)\;\;\forall(x,y)\in L\;. \tag{9}$$

3.2. Integral formulation of the problem for unidirectional flow

Using Green's second identity, homogeneous component of flow velocity (function ($\bar{c}_z(\mathbf{p})$) satisfying Laplace equation in area (Λ) limited borderline (L) can be described by the following equation (Brebbia et al 1984):

$$\bar{c}_z(\mathbf{p})=-\int_{(L)}\frac{\partial\bar{c}_z(\mathbf{q})}{\partial n_\mathbf{q}}K(\mathbf{p},\mathbf{q})\,dL_\mathbf{q}+\int_{(L)}\bar{c}_z(\mathbf{q})E(\mathbf{p},\mathbf{q})\,dL_\mathbf{q} \tag{10}$$
$$(\mathbf{p})\in\Lambda\;;(\mathbf{q})\in L$$

where $\mathbf{p}(x_\mathbf{p},y_\mathbf{p})$ and $\mathbf{q}(x_\mathbf{q},y_\mathbf{q})$ are respectively the set point and the current integration point, and function $K(\mathbf{p},\mathbf{q})$ is a fundamental solution of Laplace equation:

$$K(\mathbf{p},\mathbf{q})=\frac{1}{2\pi}\ln\left(\frac{1}{r_\mathbf{pq}}\right)\,, \tag{10a}$$

$$E(\mathbf{p},\mathbf{q})=\frac{1}{2\pi}\frac{(x_\mathbf{p}-x_\mathbf{q})\,n_\mathbf{q}^y-(y_\mathbf{p}-y_\mathbf{q})\,n_\mathbf{q}^x}{r_\mathbf{pq}^2}\,, \tag{10b}$$

where: $\mathbf{n}_\mathbf{q}=\left[n_\mathbf{q}^x,n_\mathbf{q}^y\right]=\left[\dfrac{\delta y_\mathbf{q}}{\delta L_\mathbf{q}},\dfrac{\delta x_\mathbf{q}}{\delta L_\mathbf{q}}\right]$, is a versor normal to the boundary line (L) at point $\mathbf{q}(x_\mathbf{q},y_\mathbf{q})$.

After inserting dependence (9) into integral equation (10) and separating principal value from second integral, on right-hand side due to characteristic of kernel function $E(\mathbf{p},\mathbf{q})$ on boundary line (L) when $\mathbf{p}(x_\mathbf{p},y_\mathbf{p})\equiv\mathbf{q}(x_\mathbf{q},y_\mathbf{q})$ with an assumption that the border of the area is smooth, boundary integral equation is obtained:

$$\int_{(L)}g(\mathbf{q})K(\mathbf{p},\mathbf{q})\,dL_\mathbf{q}=\Delta P\left[-\frac{1}{2}\upsilon(\mathbf{p})+\int_{(L)}\upsilon(\mathbf{q})E(\mathbf{p},\mathbf{q})\,dL_\mathbf{q}\right] \tag{11}$$

where:

$$g(\mathbf{q})=\frac{\partial\bar{c}_z(\mathbf{q})}{\partial n_\mathbf{p}}\;\text{ and }\;\upsilon(\mathbf{q})=\frac{r(\mathbf{q})^2}{4} \tag{11a}$$

Equation (9) is a Fredholm integral equation of the first kind regarding density $g(\mathbf{q})$ of the function $\bar{c}_z(\mathbf{q})$ on the boundary of the area. The integral on right-hand side with the integrand $E(\mathbf{p},\mathbf{q})$ described by dependence (8b) is understood in the meaning of Cauchy principal value.

Having solved the integral equation (11) values of function $\bar{c}_z(\mathbf{p})$ at points $\mathbf{p}(x_p, y_p)$ inside the area (Λ) are determined according to the following integral relation:

$$\bar{c}_z(\mathbf{p}) = -\int_{(L)} g(\mathbf{q})K(\mathbf{p},\mathbf{q})\,dL_{\mathbf{q}} + \Delta P \int_{(L)} \upsilon(\mathbf{q})E(\mathbf{p},\mathbf{q})\,dL_{\mathbf{q}} \quad (12)$$
$$(\mathbf{p}) \in \Lambda\,;\,(\mathbf{q}) \in L$$

The volumetric flow rate of unidirectional flow through a duct of the cross-sectional area (Λ) is equal to:

$$Q = \iint_{(\Lambda)} c_z(\mathbf{q})\,d\Lambda_{\mathbf{q}} \quad (13)$$

Substituting expressions (7) and (8) as the integrand of the equation (13) and application of Green's second identity one can obtain the expression describing the flow rate of the creeping flow in an arbitrary shape cross-section straight pipe:

$$Q = \int_{(L)} \bar{c}_z(\mathbf{q})\frac{\partial \upsilon(\mathbf{q})}{\partial n_{\mathbf{q}}}\,dL_{\mathbf{q}} - \Delta P \int_{(L)} \upsilon(\mathbf{q})\frac{\partial \bar{c}_z(\mathbf{q})}{\partial n_{\mathbf{q}}}\,dL_{\mathbf{q}}\ . \quad (14)$$

Mass flow rate of the flow is the product of the volume flow rate described by the above expression and the fluid specific weight.

3.3. Numerical solution

The simplest way of discretisation of the integral equation is to approximate the curved closed boundary line (L) with J-element system of straight line segments with central collocation points of constant function density at each element.

When the boundary line (L) of the considered area (Λ) is approximated with the boundary linear elements of the constant density of function distribution $g(\mathbf{q}_j)$ and $\upsilon(\mathbf{q}_j)$ on each element ΔL_j, the integral equation (11) is reduced to the system of (J) linear algebraic equations with unknown function $g(\mathbf{q}_j)$ at points $\mathbf{q}_j\,(j = 1,\ldots, J)$ on the edge of the area:

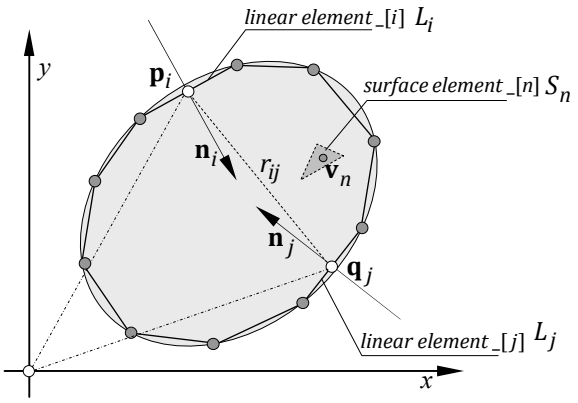

Fig. 5. Discretization of the boundary line with constant elements

$$\sum_{j=1}^{J} g(\mathbf{q}_j) \int_{(L_j)} K(\mathbf{p}_i,\mathbf{q}_j)\,dL_j =$$

$$= \Delta P\left[-\frac{1}{2}\upsilon(\mathbf{q}_i) + \sum_{\substack{j=1\\ j\neq i}}^{J} \upsilon(\mathbf{q}_j) \int_{(L_j)} E(\mathbf{p}_i,\mathbf{q}_j)\,dL_j\right] \quad (15)$$

where:

$$K(\mathbf{p}_i,\mathbf{q}_j) = \frac{1}{2\pi}\ln\left(\frac{1}{r_{ij}}\right) \quad (15a)$$

$$E(\mathbf{p}_i,\mathbf{q}_j) = \frac{1}{2\pi}\frac{(x_i - x_j)\,n_j^y - (y_i - y_j)\,n_j^x}{r_{ij}^2} \quad (15b)$$

and:

$$r_{ij} = \left[(x_i - x_j)^2 + (y_i - y_j)^2\right]^{\frac{1}{2}} \quad (15c)$$

$$\upsilon(\mathbf{q}_j) = \frac{r_j^2}{4} = \frac{1}{4}\left[(x_j - x_o)^2 + (y_j - y_o)^2\right] \quad (15d)$$

After determining the density of function distribution $g(\mathbf{q}_j)$ at the edge of the area, values of the function $\bar{c}_z(\mathbf{p}_n)(n = 1,\ldots,N)$ at points $(\mathbf{p}_n)(n = 1,\ldots,N)$ inside the area (Λ) are calculated using the following relation:

$$\bar{c}_z(\mathbf{p}_n) = \sum_{j=1}^{J} g(\mathbf{q}_j) \int_{(L_j)} K(\mathbf{p}_n,\mathbf{q}_j)\,dL_j +$$

$$+\sum_{\substack{j=1\\ j\neq i}}^{J} \upsilon(\mathbf{q}_j) \int_{(L_j)} E(\mathbf{p}_n,\mathbf{q}_j)dL_j \quad (16)$$

Finally, the velocity $c_z(\mathbf{p}_n)(n = 1,\ldots,N)$ at the points $(\mathbf{p}_n)(n = 1,\ldots,N)$, according to the equation (7), is described by the following sum:

$$c_z(\mathbf{p}_n) = \bar{c}_z(\mathbf{p}_n) + \Delta P\,\upsilon(\mathbf{p}_n) \quad (n = 1,\ldots,N) \quad (17)$$

3.4. Velocity field in elliptical, rectangular and triangular cross-section straight tubes – calculations principles

The flow velocity field is determined for the flow through straight pipe or closed duct thoroughly filled with liquid of density ρ=1000.00 kg/m^3, and viscosity μ=1.00*10^{-3} Pa·s (ethylene glycol 20% H_2O) at temperature 80°C) and pressure difference ΔP=10.00 s^{-1}m^{-1}.

3.4.1 Flow through an elliptic cross-section duct

The flow velocity field is determined for elliptic dust of the following dimensions: a=0.050 m, b=0.025 m. The results of the calculations are presented graphically in Fig. 6.a – c.

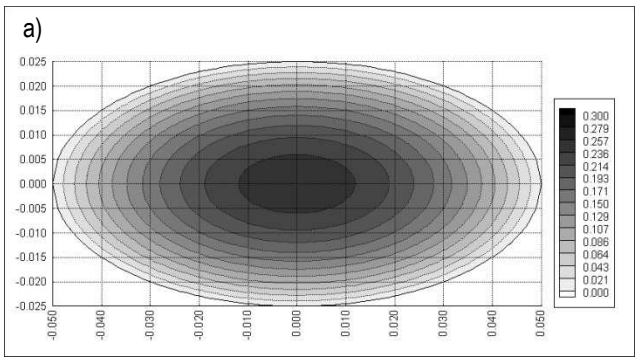

Fig. 6. Velocity distribution in a straight duct of elliptical cross-section:
a) Contour line chart of the velocity field in the duct
b) Velocity chart in the cross-sections: x=const
c) Velocity profile

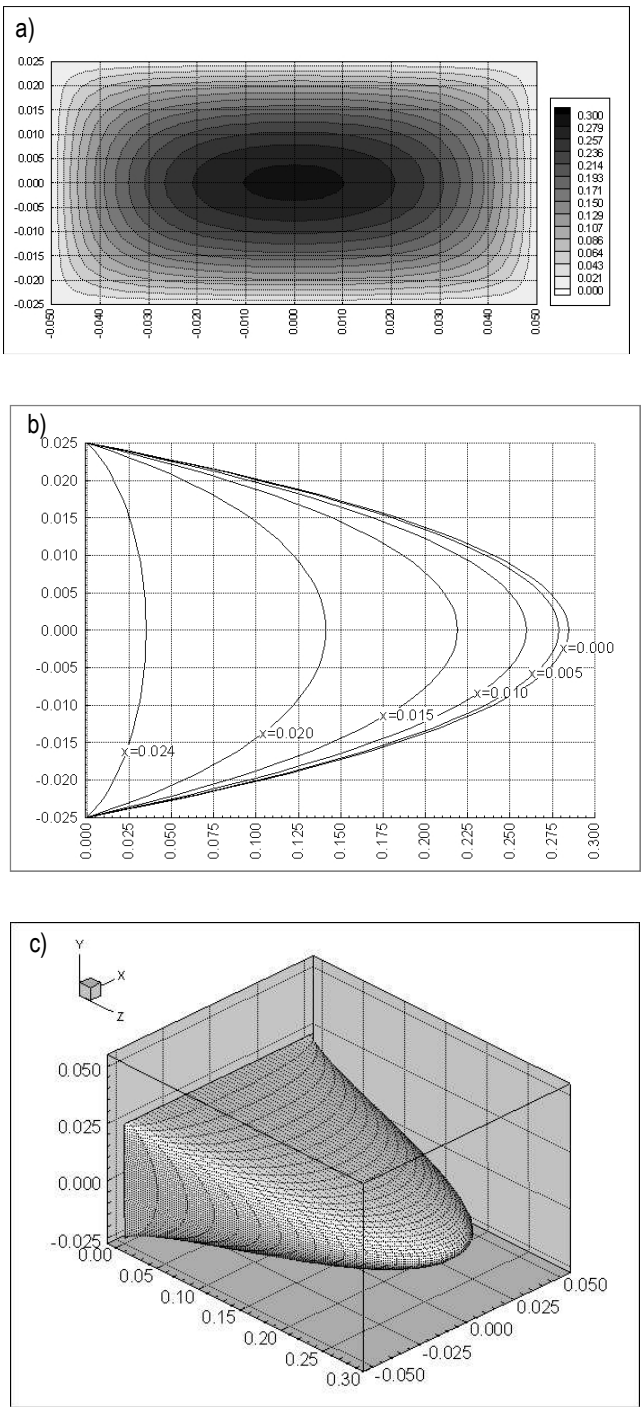

Fig. 7. Velocity distribution in a rectangular cross-section duct:
a) Contour line chart of the velocity field in the duct
b) Velocity chart in the cross-sections: x=const
c) Velocity profile

3.4.2. Flow through a rectangular cross-section duct

The flow velocity field is determined for rectangular duct of edges dimensions: a=0.050 m, b=0.025 m. The results of the calculations are presented graphically in Fig. 7.a – c.

3.4.3. Flow through a triangular cross-section duct

Velocity field is determined in the duct of a triangular cross-section (equilateral) of side size a=0.050 m.

The results of the calculations are presented graphically in Fig. 8.a – c.

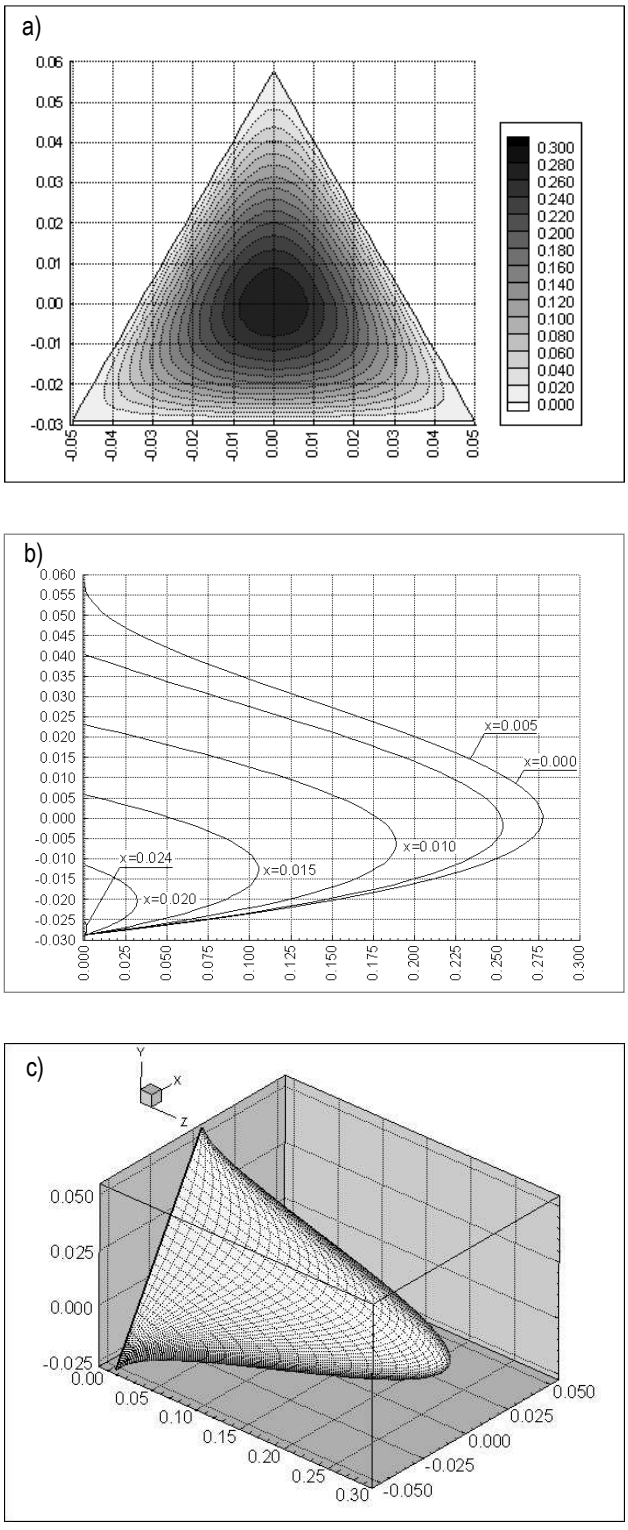

Fig. 8. Velocity distribution in a triangular cross-section duct.
a) Contour line chart of the velocity field in the duct
b) Velocity chart in the cross-sections: x=const
c) Velocity profile

4. CONCLUSIONS

The article presents classic model of calculations of temperature distribution in the absorber plate and in the pipe system in a flat plate solar collector. Further in the paper it is shown, how an energy efficiency of the device is determined. The model describes phenomena of flow and convective heat transfer in the systems of pipes of circular cross-sections. Determining velocity fields and temperature fields in the flow systems of liquid collectors is the principal element of flow and thermal optimisation of solar collectors.

The presented method uses Boundary Element Method that enables modelling and determining of flows in solar collectors pipe systems where cross-section shapes are different from circular. The method offers the possibility of determining velocity field and flow rate in the laminar flow of viscous fluid through straight-axis pipes and closed channels of arbitrary cross-section shape.

REFERENCES

1. **Alvarez A., Cabeza O., M.C. Muñiz M.C., Varela L.M.** (2010), Experimental and numerical investigation of a flat-plate solar collector, *Energy,* 35, 3707-3716.
2. **Batchelor G.K.,** (1967), *An Introduction to Fluid Dynamics*, Cambridge Univ. Press.
3. **Brebbia K., Telles, J.C.F., Wrobel, L.C.** (1984), Boundary Element Techniques. Theory and Applications in Engineering, *Springer-Verlag*.
4. **Charalambous P.G., Maidment G.G., Kalogirou S.A., Yiakoumetti K.** (2007), Photovoltaic thermal (PV/T) collectors: A review, Applied *Thermal Engineering,* 27, 275-287.
5. **Chwieduk D.** (2011), *Solar Energy in Buildings (in Polish),* Arkady.
6. **Farahat S., Sarhaddi F., Ajam H.** (2009), Exergetic optimization of flat plate solar collectors, *Renewable Energy*, 34, 1169–1174.
7. **Herrero Martín R., Pérez-García J., García A., García-Soto F.J., López-Galiana E.** (2011), *Simulation of an enhanced flat-plate solar liquid collector with wire-coil insert devices*, Solar Energy, 85, 455–469.
8. **Ibrahim A., Othman M.Y., Ruslan M.H., Mat S., Sopian K.** (2011), Recent advances in flat plate photovoltaic/thermal (PV/T) solar collectors, *Renewable and Sustainable Energy Reviews*, 15, 352-365.
9. **Kalogirou S.A.** (2004), Solar thermal collectors and applications, *Progress in Energy and Combustion Science*, 30, 231–295.
10. **Luminosu I., Fara L.** (2005), Determination of the optimal operation mode of a flat solar collector by exergetic analysis and numerical simulation, *Energy*, 30, 731–747.
11. **Vestlund J., Rönnelid M., Dalenbäck J.O.** (2009), Thermal performance of gas-filled flat plate solar collectors, *Solar Energy*, 83, 896–904.
12. **Zhang X., Xudong Zhao X., Smith S., Xu J., Yuc X. (**2012), Review of R&D progress and practical application of the solar photovoltaic/thermal (PV/T) technologies, *Renewable and Sustainable Energy Reviews,* Vol. 16, 594-617.
13. **Zondag H. A.** (2008)**,** Flat-plate PV-Thermal collectors and systems: A review, *Renewable and Sustainable Energy Reviews,* 12, 891–959.

Acknowledgement: The work described in this article was supported by Bialystok University of Technology Research Project S/WBiIŚ,5/11.